Agricultural Water Management 243 (2021) 106390

Contents lists available at ScienceDirect

Agricultural Water Management

journal homepage: www.elsevier.com/locate/agwat

# Effectiveness of a subsurface irrigation system with ceramic emitters under low-pressure conditions

Yaohui Cai[a,b,c], Chunping Yao[b], Pute Wu[a,b,c,*], Lin Zhang[a,b,c], Delan Zhu[b,c], Junying Chen[b,c], Yichao Du[a]

[a] Institute of Soil and Water Conservation, Northwest A&F University, Yangling, 712100, China
[b] Key Laboratory of Agricultural Soil and Water Engineering in Arid and Semiarid Areas, Ministry of Education, Northwest A&F University, Yangling, 712100, China
[c] Institute of Water-saving Agriculture in Arid Areas of China, Northwest A&F University, Yangling 712100, China

ARTICLE INFO

*Keywords:*
Uniformity
Irrigation quality
Emitter
Subsurface irrigation
Discharge

ABSTRACT

A subsurface irrigation system with ceramic emitters (SICE) without a pump has been developed to limit energy consumption and reduce greenhouse gas emissions. Yet whether SICE can be used in low-pressure conditions has not been tested; moreover, there is no index for evaluating the irrigation quality of SICE. Laboratory experiments, with six treatments, were conducted to study ceramic emitter hydraulic characteristics in the air and soil under different working pressure heads and emitter types. The results indicated that when $H$ increased, the emitter discharge increased linearly, and the discharge deviation decreased in the air. With increased $H$ in the soil, the emitter discharge, soil water content, and soil water content uniformity increased, and the discharge deviation decreased. When $H$ was greater than or equal to 20 cm, the discharge deviation in the soil was less than that in the air, and the soil water content uniformity was higher than 80 %. The soil water content uniformity could be used in the evaluation of the irrigation quality of SICE based on the reliability and convenience of observation. To make the best use of soil water potential on the outflow of the emitter, reduce the discharge deviation, and improve soil water content uniformity, the working pressure head of SICE should be higher than 20 cm.

## 1. Introduction

Water-saving irrigation technology could improve crop yields and reduce labor intensity, but it also requires high energy inputs and may cause environmental problems (Adu et al., 2019; Sampson and Perry, 2019; S. Wang et al., 2019; W. Wang et al., 2019). Kaltsas et al. (2007) reported that irrigation energy demand accounted for approximately 21 % of the total energy consumption in conventional olive orchards. Todde et al. (2019) found that the application of photovoltaic irrigation systems would decrease energy consumption 41 % and 67 % in Morocco and Portugal, and avoid the emission of large amounts of greenhouse gases. Romero-Gamez et al. (2017) showed that the greatest environmental impact was from an intensively irrigated-integrated system and a super-intensive irrigated-integrated system because of the electricity consumed during irrigation. Pumps consume most of the electricity in irrigation systems (Powell et al., 2019). To reduce energy consumption and greenhouse gas emissions, an irrigation system that requires a lower working pressure head ($H$), and can function without a pump, would benefit the industry.

Pitcher or pot irrigation is a traditional irrigation method used to supply water to crops without external inputs (such as oil and electricity) under drought conditions in arid regions, for which $H$ is usually lower than 20 cm (Paredes and San Jose, 2019; Siyal et al., 2009). Singh and Ghosal (2015) argued that the interaction of pitcher fertigation brought a 106.9 % and 13.5 % increase in lac crop yield ratio of Ber (*Ziziphus mauritiana*) in summer and winter, respectively. Pachpute (2010) used a suite of water management practices, including a pitcher irrigation method, as well as water conservation techniques of manure application and mulching, in North-Eastern Tanzania, that led to an increase (203 %) in total cucumber yield. Batchelor et al. (1996) found that subsurface irrigation with clay pipes was particularly effective in improving yields, crop quality, and water use efficiency, as well as being inexpensive, simple, and easy-to-use (in southeast Zimbabwe and northern Sri Lanka). However, irrigation of crops with pitchers or ceramic tubes is seldom scaled up in modern field conditions (Bainbridge, 2001). One problem is that pitchers are difficult to connect to large-scale irrigation systems (Pachpute, 2010). The other is that discharges and manufacturing deviations of devices are difficult to

* Corresponding author at: No. 22, Xinong Road, Yangling, Shaanxi, 712100 China.
*E-mail addresses:* gjzwpt@vip.sina.com, caiyh@nwafu.edu.cn (P. Wu).

https://doi.org/10.1016/j.agwat.2020.106390
Received 10 February 2020; Received in revised form 5 July 2020; Accepted 11 July 2020
Available online 09 August 2020
0378-3774/ 

precisely control (Hajjaji and Mezouari, 2011; Naik et al., 2013). Therefore, to meet modern irrigation requirements, optimized pitcher structures and material properties are needed.

A subsurface irrigation system with ceramic emitters (SICE) recently has been developed (Cai et al., 2017). Most of the components of SICE are similar to a subsurface drip irrigation system (SDI) (Camp, 1998; Lamm and Trooien, 2003); it eliminates the need for pumps, as irrigation water is supplied by a water tank of constant pressure. Such a SICE works with low pressure, small discharge, and continuously, which would maintain a suitable root-zone and soil-water content, thus maintaining water availability to plants (Lazarovitch et al., 2006). The $H$ of a ceramic emitter is usually smaller than 100 cm, and it can be close to zero or negative (Ashrafi et al., 2002). Li et al. (2019) found that negative pressure water supply not only maintained a high fruit yield but also significantly increased water use efficiency. Nalliah and Ranjan (2010) stated that a capillary-irrigation technique (with porous membranes with different negative pressures) offered precise water delivery with minimal labor requirements, suitable for use in greenhouse pepper production. However, in field environments, the conditions in which an $H$ of zero or negative seldom occur, unless there is a special water supply to provide water for the emitter (Li et al., 2017). Cai et al. (2018) suggested that the $H$ of ceramic emitter should be higher than 20 cm under field conditions to reduce system costs. Yet, this conclusion was just assumed based on previous observations. Therefore, a critical question remains: can a SICE be used with $H$ lower than 20 cm?

In a SICE, ceramic emitters are used in place of traditional plastic emitters. There are many advantages of ceramic emitters over pitchers, such as controllable emitter discharge and environmental safety (Cai et al., 2017). However, large manufacturing deviations are a prominent feature of ceramic products. To reduce manufacturing deviations of ceramics, researchers have adopted various methods, such as droplet jetting, slurry-curing procedures (Cai et al., 2019a), and frozen slurry-based laminated-object manufacturing processes (Zhang et al., 2018). However, in most developing countries, it is difficult to prepare ceramic emitters (pitchers, pots) with low manufacturing deviation because ceramic emitters are typically made by hand (Siyal et al., 2009; Vasudevan et al., 2011). Much of the research on the performance of SDI systems in the last two decades has focused on how the interaction between the effects of emitter discharge and soil properties could affect irrigation uniformity (Lazarovitch et al., 2006). Gil et al. (2008) found that irrigation uniformity of SDI non-compensating emitters to be greater than surface drip irrigation due to the interaction between the effects of emitter discharge and soil pressure. Ren et al. (2017) stated that the greater the initial water content, soil bulk density, and mass fractal dimension, the smaller the deviation rate of lateral flow of an SDI. The emitter discharge exponent of the ceramic emitter in the SICE system is 1, and thus it is a non-compensating emitter (ASABE, 2006; Cai et al., 2019b); however, the $H$ and discharge of SICE are lower than for SDI. As such, can soil properties affect irrigation uniformity of SICE, especially for ceramic emitters with large manufacturing deviations?

The present study aimed to (1) compare emitter discharge, and discharge deviations in the air and soils, under different $H$ and emitter types, (2) select a suitable indicator for evaluating irrigation quality of SICE, and (3) identify a working pressure head for SICE.

## 2. Materials and methods

### 2.1. Emitter hydraulic characteristics in the air

#### 2.1.1. Experimental setup

The experiment setup had eight major components: water tank, pump, manometer, branch, lateral, ceramic emitters, beakers, and manometer (Fig. 1). Five ceramic emitters were installed on one lateral, and the emitter spacing was 0.20 m. Five laterals were connected by a branch (total emitter n = 25), and the branch was fed by the water tank and pump. The emitter discharge under different $H$ was observed and recorded; emitter discharge was measured by the weighing method and taken as the average of 25 replicates. The irrigation water used in the experiment was urban domestic water from Yangling, and the water temperature during the test was 20 ± 3 °C.

In the experiment, ceramic emitters with two different porosities were employed, which were denoted as CE1 and CE2. The ceramic emitters were made of silica, talc, and silica sol, and then sintered in a tunnel furnace. The porosity of the ceramic emitters was controlled by altering the grain size of the silica. The external diameter, internal diameter, inner hole depth, and height of ceramic emitters were 39.37 mm, 19.82 mm, 4.97 mm, and 6.80 mm, respectively. The open porosity of CE1 and CE2 were 0.36 and 0.28, respectively.

#### 2.1.2. Calculated method

Flow velocity of the fluid through the porous materials can be calculated by obtaining the relation between the pressure drop and hydraulic conductivity of the porous materials (Wu et al., 2018). As the ceramic emitters are made of porous ceramics, and we assume that the ceramic emitter is always saturated during irrigation. Therefore, laminar flow occurs in the pore, and Darcy's law, which describes a linear relationship between pressure gradient and the fluid velocity is reliable (Li et al., 2019a, 2019b):

$$v = \frac{Q}{A} = k\frac{dH}{dL} \tag{1}$$

where $\frac{dH}{dL}$ is the pressure gradient along the fluid direction, $v$ is the fluid velocity calculated by the emitter discharge divided by seepage area, $k$ is the emitter hydraulic conductivity, $Q$ is emitter discharge, $A$ is emitter seepage area.

For the fluid that cannot be compressed, the pressure gradient can be calculated as:

$$\frac{dH}{dL} = \frac{H_{\mathrm{in}} - H_{\mathrm{out}}}{L} \tag{2}$$

where, $H_{\mathrm{in}}$ is the pressure of water at the ceramic emitter entrance, and in most cases, $H_{\mathrm{in}}$ is equal to the working pressure $H_{\mathrm{w}}$; $H_{\mathrm{out}}$ is the pressure of water at the ceramic emitter exit, when the ceramic emitter is working in air, $H_{\mathrm{out}} = 0$; $L$ is the seepage tracking.

Therefore, the emitter discharge in air could be expressed as:

$$Q = \frac{kAH_{\mathrm{w}}}{L} \tag{3}$$

However, for some types of porous media with small pore size, such as fine-grained soil, sandstones, fluids can flow through these porous media only if the fluid force is sufficient to overcome the threshold pressure gradient (Wang et al., 2019; Wang et al., 2019; Min et al., 2018; Liu and Birkholzer., 2012). Prada and Civan (1999) studied the permeability of saturated brine in eight typical sandstones and Brown sandstones, and found the permeation of saturated brine was not consistent with Darcy's law. There was an initial pressure gradient, which is the function of the permeability of pore medium and the viscosity coefficient of the fluid. Therefore, Eq. (3) would be:

$$Q = \frac{kA(H_{\mathrm{w}} - H_{\mathrm{i}})}{L} \tag{4}$$

where $\frac{H_{\mathrm{i}}}{L}$ is initial pressure gradient.

For ceramic emitter, the emitter discharge would not be negative value, and for a certain porous medium, the initial pressure $H_{\mathrm{i}}$ is constant value, therefore, Eq. (4) would be:

$$\begin{aligned} &Q = 0 && H_{\mathrm{w}} \le H_{\mathrm{i}} \\ &Q = k\frac{(H_{\mathrm{w}} - H_{\mathrm{i}})\cdot A}{L} = k\frac{H_w \cdot A}{L}\text{-i} = k\frac{H_w \cdot A}{L}\text{+C} && H_{\mathrm{w}} > H_{\mathrm{i}} \end{aligned} \tag{5}$$

where, i and C are constant values.

For a ceramic emitter for which structure parameters and ceramic characteristics are fixed values, the emitter seepage area $A$, seepage

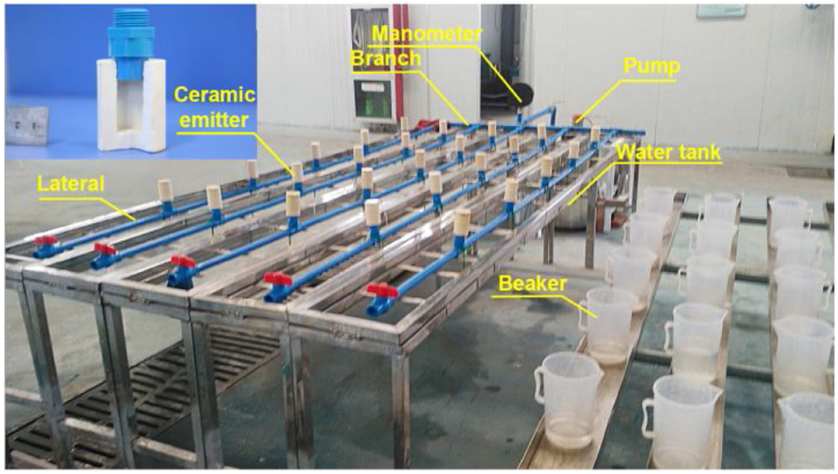


**Fig. 1.** The experimental setup of the emitter hydraulic characteristics test.

tracking $L$, and hydraulic conductivity $k$ are constants, and therefore, Eq. (5) can be re-written as:

$$Q = 0 \quad H_w \le H_i$$
$$Q = KH_w + C \quad H_w > H_i \tag{6}$$

where $K$ is the emitter discharge coefficient.

Due to various factors, such as manufacturing-specific processes and material deformation, the emitter will inevitably produce deviations. In the present experiments, the lateral length was just 2 m, the discharge deviation caused by hydraulic deviation was negligible, so the emitter discharge variation in the air would be equal to the emitter manufacturing variation. The calculation of manufacturing variation $CV_m$ is given in Eq. (7):

$$CV_m = \sqrt{\frac{1}{n-1}\frac{(Q_x - \bar{Q}^2)}{\bar{Q}^2}} \tag{7}$$

where $Q_x$ is the $x$th emitter discharge in the air; $\bar{Q}$ is average emitter discharge under the same $H$; and $n$ is the total number of emitters (25).

The evaluation standards of $CV_m$, listed by the American Society of Agricultural and Biological Engineers, are shown in Table 1.

**Table 1**
Classifications of manufacturer's coefficient of variation, $CV_m$, for emitters.

| $CV_m$/% | < 5 | 5 − 7 | 7 − 11 | 11 − 15 | > 15 |
|---|---|---|---|---|---|
| Classification | Excellent | Average | Marginal | Poor | Unacceptable |

Adopted from ASABE (2006).

### 2.2. Emitter hydraulic characteristics in the soil

#### 2.2.1. Experimental setup

The experiment setup had eight major components: constant pressure water tank, pressure sensors, laterals, intake microtubules, drainage microtubules, ceramic emitters, soil pots, and balance (Fig. 2). The laboratory experiments were performed in five soil pots (Volume = 17.24 L) made of plastic, with the pot spacing 35 cm. Ceramic emitters were fed by the constant pressure water tank. In each pot, only one ceramic emitter was installed at a depth of 15 cm, and it was connected to the lateral with a 4-mm rubber intake microtubule. At the beginning of the experiment, a rubber drainage microtubule was connected to the headcover of the ceramic emitter to exhaust air in the lateral and microtubule.

#### 2.2.2. Soil sample

After sieving using a 2 mm mesh-sieve, the air-dried soil with an average soil bulk density of 1.3 g $cm^{-3}$ was used to fill the soil tank. Clay loam (33.1 % clay, 26.8 % silt, and 40.1 % sand, USDA soil taxonomy) was selected for the study. The procedure for filling the pots was first to feed the ceramic emitter and rubber pipe through the right side and the loading and compaction 5-cm layers of soil to each pot. To avoid soil stratification, the upper surface of each layer was ensured to be sufficiently rough. The cumulative infiltration of the emitter was obtained by weighing the soil pot at intervals of 10 min for the first 1 h, and then at intervals of 30 min for the last 5 h. The cumulative infiltration of the ceramic emitter may be affected by various parameters, but experiments were implemented specifically to study the effect of $H$ and emitter type on emitter infiltration characteristics of the soil. The input data of experiments are listed in Table 2.

#### 2.2.3. Calculated method

The relationship between cumulative infiltration and time can be described by a power function (Su et al., 2016):

$$I = at^b + c \tag{8}$$

where $I$ is the cumulative infiltration at time $t$, and $a$, $b$, and $c$ are the coefficients.

Therefore, the emitter discharge in the soil or infiltration rate could be obtained by Eq. (7):

$$q = i = \frac{dI}{dt} = abt^{b-1} \tag{9}$$

System uniformity is ordinarily defined in terms of the variation of $q$ from emitter to emitter, and the coefficient of variation ($CV_q$) of emitters buried in the soil can also be calculated by Eq. (5). When ceramic emitters are buried in the soil, emitter discharge is not easily measured, and thus system uniformity is difficult to calculate. Therefore, soil water content uniformity may be much easier to observe than that of emitter discharge. Christiansen soil water content uniformity ($CU_\theta$) may be expressed by (Christiansen, 1941):

$$CU_\theta = 1 - \frac{1}{n}\sum_{x=1}^{n}\frac{|\theta_x - \bar{\theta}|}{\bar{\theta}} \tag{10}$$

where $\theta_x$ is the $x$th soil water content in the soil pot and $\bar{\theta}$ is the average soil water content of a total of 5 pots.

The evaluation standards of $CU_\theta$, listed by the American Society of Agricultural and Biological Engineers, are shown in Table 3.

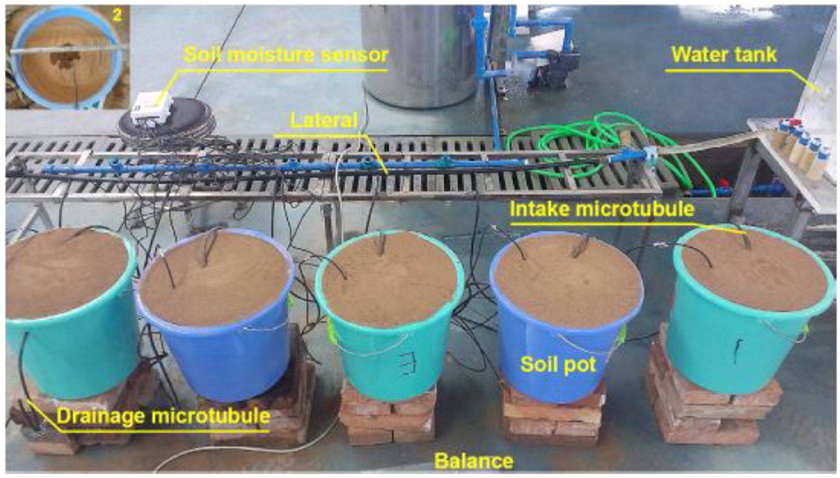


**Fig. 2.** The SICE infiltration experimental setup.

**Table 2**
Parameters used in experiments.

| Treatment | 1 | 2 | 3 | 4 | 5 | 6 |
|---|---|---|---|---|---|---|
| *H* (cm) | 10 | 20 | 50 | 10 | 20 | 50 |
| Emitter type | CE1 | CE1 | CE1 | CE2 | CE2 | CE2 |

**Table 3**
The evaluation standards of $CU_\theta$.

| $CU_\theta$/% | > 90 | 80 − 90 | 70 − 80 | 60 − 70 | < 60 |
|---|---|---|---|---|---|
| Classification | Excellent | Good | Moderate | Weak | Unacceptable |

Adopted from ASABE (2006).

## 3. Results

### 3.1. Emitter hydraulic characteristics in the air

#### 3.1.1. Emitter discharge in the air

Fig. 3 shows the emitter discharge at different *H* in the air. A linear relationship is observed between the emitter discharge and *H*. For example, as *H* increases from 10 cm to 70 cm, the discharge of CE1 increases from 0.20 L h$^{-1}$ to 1.74 L h$^{-1}$. When *H* is higher than 3.26 cm, *H* and *Q* conform to the relationship of $Q$ = 0.027$H$ - 0.088. Also, when the porosity of the emitter increases, the emitter discharge increases. More importantly, the initial working pressure head of each emitter is different, the initial working pressure head of CE 1 ranges from −0.01 cm –6.56 cm, and -0.19 cm to 8.26 cm for CE2. This indicates that the emitter discharge under low-pressure conditions may vary substantially.

#### 3.1.2. Discharge deviation in the air

Fig. 4 shows the $CV_m$ at different *H*. As *H* increases, the discharge deviation in the air of both emitters decreases, and the relationship between $CV_m$ and *H* is a logarithmic function. For example: when *H* increases from 10 cm to 70 cm, the discharge deviation of the CE1 decreases from 38.90 % to 20.84 %, and they fit into a functional relationship of $CV_m = 61.61 - 9.40\ln(1.33 + H)$. The ceramic emitter is a porous structure. According to Eq. (6), only when the hydraulic gradient exceeds the initial hydraulic gradient can the emitter seep normally. Under low-pressure conditions, the complex pore structure causes the water flow inside the emitter to be chaotic, so a small pore deviation may cause a large discharge deviation. However, when the working pressure head is high, the porous medium can flow normally, and the discharge deviation will not be particularly large.

The discharge deviations of these emitters are all higher than the specified value (15 %) when *H* is smaller than 70 cm (Table 1); therefore, these emitters cannot be used according to ASABE regulations. However, when *H* increases, the emitter discharge deviation decreases. For example, when the working pressure head of CE1 is 411 cm, the discharge deviation is 5.0 % and CE1 can be considered as an

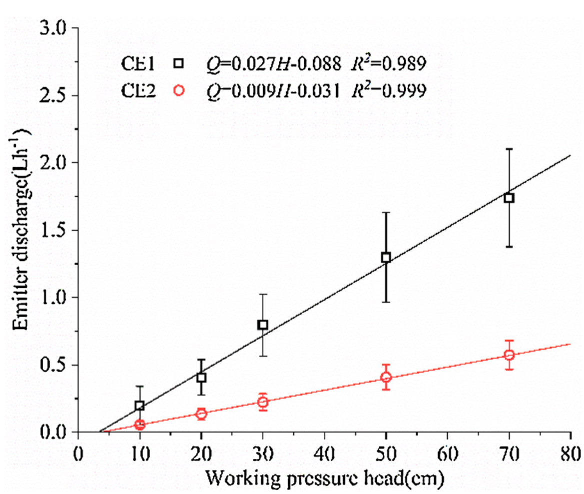


**Fig. 3.** Relationship between emitter discharge in the air and *H*.

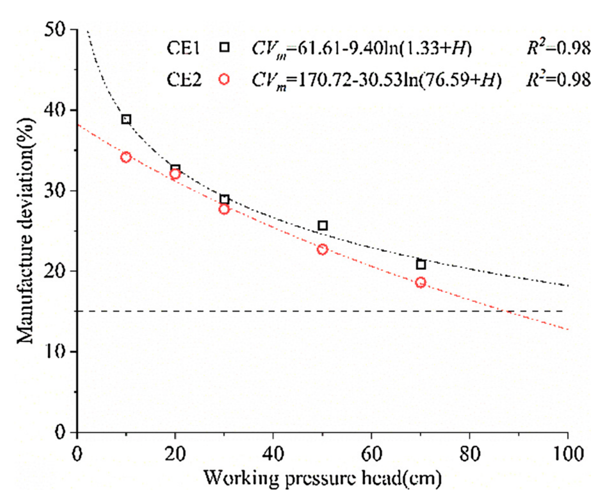


**Fig. 4.** Relationship between $CV_m$ and *H*.

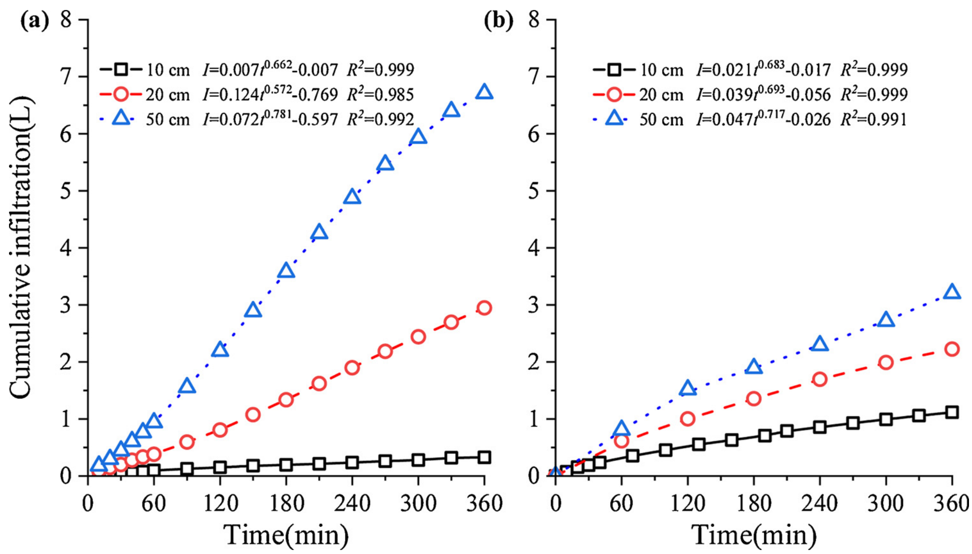


**Fig. 5.** Cumulative infiltration as a function of time at different $H$ and emitter types ((a). CE1, (b). CE2).

"excellent" product according to ASABE regulations. When the working pressure head reaches 151 cm, the discharge deviation can be 5.0 % for CE2. Therefore, if the emitter discharge deviation smaller than 11 %, the emitters can be used in the field. Based on Fig. 4, the working pressure head must be higher than a specific value, 215 cm for CE1 and 110 cm for CE2.

### 3.2. Emitter hydraulic characteristics in the soil

#### 3.2.1. Emitter discharge in the soil and soil water content

Fig. 5 shows the change of cumulative infiltration with time at different $H$ and emitter types over 360 min. As time and $H$ increases, the cumulative infiltration increases. For example, when the irrigation time of CE1 is 360 min, the cumulative infiltration under $H$ of 50 cm is 20.58 times than that of 20 cm; it is 5.88 times for CE2 under the same conditions. As in the air, with the same $H$, the cumulative infiltration of CE1 is significantly greater than that of CE2. For example, when $H$ is 20 cm, the cumulative infiltration of CE1 is 1.90 L, and that of CE2 is just 0.20 L. However, the cumulative infiltration of CE1 under 10 cm is unusual—this may be due to the inadequate contact between the emitter and the surrounding soil and then a large positive pressure is generated by the irrigation water surrounding the emitter leading to a smaller cumulative infiltration.

Eq. (6) is used to fit the relationship between cumulative infiltration volume ($I$) and time ($t$) under different emitter types and $H$. The formulas are shown in Fig. 5. As can be seen from these formulas, the index $b$ is in the range of 0.57–0.78, and it shows that the rate of cumulative infiltration would gradually decrease with time. The relationship of the emitter discharge (infiltration rate) in the soil over time can be obtained by taking the derivative of these formulas (Fig. 6).

It can be seen from Fig. 6 that emitter discharge is larger than that in the air at first. With increased time, the emitter discharge gradually decreases and stabilizes. For example, when $H$ of CE2 is 10 cm, the discharge decreases from 0.41 L $h^{-1}$ to 0.13 L $h^{-1}$. $H$ has a strong influence on emitter discharge, but the emitter discharge is quite different from that in the air and this is mainly due to the influence of soil water potential. From Eq. (6), the emitter discharge in the soil could be calculated by Eq. (11):

$$Q = K(H_w - \varphi) + C \tag{11}$$

where $\varphi$ is the soil water potential around the ceramic emitter.

When $H$ is greater than 0 cm, the emitter discharge is determined by $H$ and soil water potential around the ceramic emitter. Moreover, the soil water potential changes from negative to zero, or even positive, when irrigation water enters the soil. When irrigation begins, the soil water content is less than the saturated water content, the soil water potential is matric potential, and it is a negative value. Therefore, the emitter discharge in the soil would be greater than that in the air, and soil water potential could promote the outflow of the emitter. Subsequently, the soil water potential increases gradually with increasing soil water content. The relationship between soil matric potential and soil water content is expressed by the V-G equation (van Genuchten, 1980):

$$\varphi = -\frac{1}{\alpha}\left[\left(\frac{\theta_s - \theta_r}{\theta - \theta_r}\right)^{\frac{1}{m}} - 1\right]^{\frac{1}{n}} \tag{12}$$

where $\theta$ is soil water content, $\theta_s$ is soil saturated water content, $\theta_r$ is soil residual water content, $n$ and $m$ are fitting parameters, $m = 1-1/n$, and $\alpha$ is the parameter related to soil physical properties.

From Eqs. (11) and (12), we can obtain the emitter discharge as:

$$q = K(H_w + \frac{1}{\alpha}\left[\left(\frac{\theta_s - \theta_r}{\theta - \theta_r}\right)^{\frac{1}{m}} - 1\right]^{\frac{1}{n}}) + C \tag{13}$$

It can be seen from Eq. (13) that higher the soil water content, lower the emitter discharge. Fig. 6 shows the change of the average soil water content in the soil pots at different $H$ and emitter types over 360 min. The changes in the soil water content are similar under different treatments, and the soil water content increases gradually with time. The higher the $H$, the faster the soil water content increases. When $H$ of CE1 is 50 cm, the soil water content reached the saturated water content in 360 min. In general, the soil water content of CE1 is higher than that of CE2. However, the situation is reversed when $H$ is 10 cm, as the soil water content of CE2 is higher than that of CE1. This is because there was a large discharge difference of CE1 when $H$ is 10 cm, and the discharges in the soil of the three emitters were almost equal to 0 L $h^{-1}$. Therefore, the soil water content of these three replicates is slightly higher than the initial soil water content.

At 360 min, the relationship between the emitter discharge in the soil and air is shown in Fig. 7. It can be seen the larger $H$ and discharge coefficients, the larger the emitter discharge in the soil. However, emitter discharge in the soil at 360 min of CE1 is less than its discharge in the air; conversely, it is greater than in the air for CE2. When $H$ is 10 cm, some emitters of CE1 and CE2 failed to flow normally, which may influence experimental results.

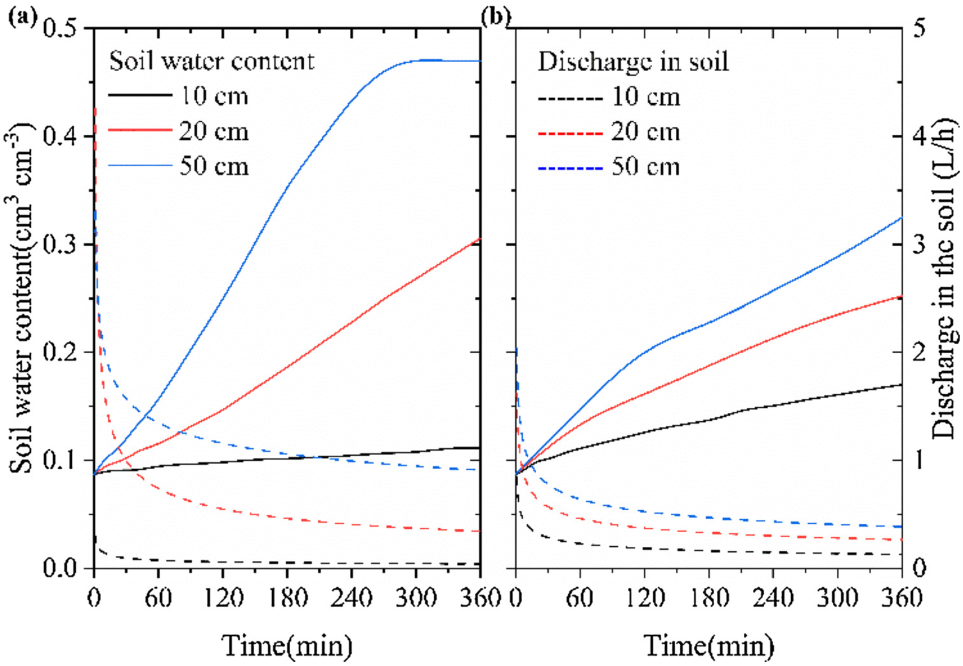


**Fig. 6.** Emitter discharge in the soil and soil water content as a function of time at different *H* and emitter types ((a). CE1, (b). CE2).

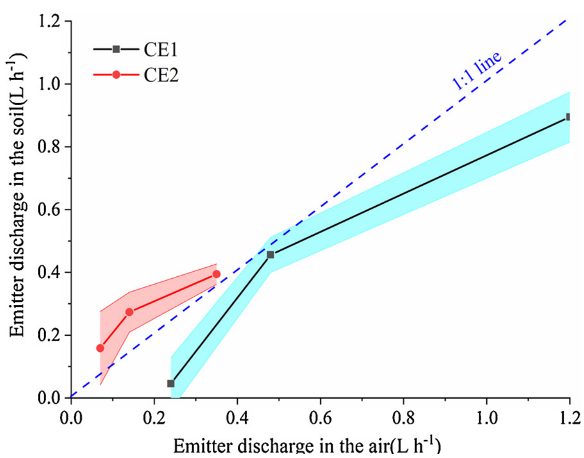


**Fig. 7.** Emitter discharge in the air and soil at 360 min.

However, when the emitter discharge coefficient is larger (such as in CE1), water would quickly enter the soil, and the soil water content would reach saturated water content rapidly. Therefore, the matric potential would become 0, and the soil hydraulic conductivity would be the saturated hydraulic conductivity ($K_s$). If the emitter discharge per unit area ($Q'$) is greater than $K_s$, positive pressure will be generated in the soil around the emitter, and soil would inhibit the outflow of the emitter. Therefore, the emitter discharge gradually decreases, and the discharge in the soil would be a stable value less than the emitter discharge in the air. According to Shani et al. (1996), based on the research of subsurface drip irrigation, the positive pressure at the orifice of emitter conformed to the following relationship:

$$\varphi = \left(\frac{2-\alpha\cdot r_0}{8\pi\cdot K_s\cdot r_0}\right)\cdot Q' - \frac{1}{\alpha_G} \tag{14}$$

where $r_0$ is the radius of the saturated zone and $\alpha_G$ is the parameter for the unsaturated hydraulic conductivity from Gardner's equation (Gardner, 1958).

Combining Eq. (11) and (14), the steady emitter discharge is:

$$q = K\left(H_w + \frac{1}{\alpha_G} - \frac{2-\alpha r_0}{8\pi K_s r_0}\cdot\frac{KH_w}{S}\right) + C \tag{15}$$

where $S$ is the external surface area of the emitter.

According to Eqs. (14) and (15), it can be seen the soil water content outside the emitter is less than the saturated water content at the beginning of infiltration, and the soil water potential is the negative matric potential. Therefore, soil water potential can promote the outflow of the emitter, and the emitter discharge is greater than that in the air. The soil water potential increases gradually with the increase of water content, until reaching saturation. When the soil water content reaches saturation, the soil water potential outside the emitter becomes 0, so the emitter discharge in the soil is equal to the discharge in the air. When irrigation water continues entering the soil, $K_s$ has been saturated hydraulic conductivity. Therefore, a saturation zone is formed, positive pressure generates around the emitter, and the emitter discharge would continue to decrease and eventually stabilize. When the emitter discharge coefficient is small (such as for CE2), $Q'$ is smaller than the unsaturated hydraulic conductivity $K(\theta)$ of soil, and soil would be no longer restrain the outflow of the emitter. Therefore, emitter discharge would be a function of soil water potential, and the emitter discharge in the soil would be larger than that in the air.

#### 3.2.2. Discharge deviation in the soil and soil water content uniformity

Fig. 8 shows the variation of the discharge deviation rate in the soil over time under different types of emitters and *H*. It can be seen the higher *H* of the emitter, the smaller the discharge deviation in the soil. When *H* is 10 cm, discharge deviations in the soil are greater than 100 % for CE1 and CE2, especially the discharge deviation of CE1 that increases gradually with time. Vasudevan et al. (2014) found that there was an additional flow due to the water deficit in the soil. This is a negative pressure or an equivalent negative hydraulic head. As a result of soil water potential, the emitter discharge will produce certain changes compared with that in the air. In the soil, the emitter discharge is determined by both the working pressure head and soil water potential (soil water content), as the water content increases, the effect of soil will be weakened. However, the emitter discharge deviations of CE1 and CE2 under 10 cm is different from other treatments. This may be due to the inadequate contact between the emitter and the surrounding soil. Some emitters would not work normally, the emitter

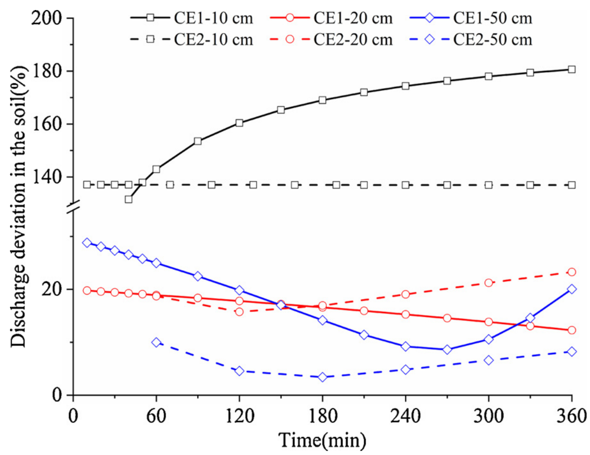


**Fig. 8.** Discharge deviation in the soil as a function of time at different *H* and emitter types.

discharge is nearly 0 L $h^{-1}$, the emitter discharge deviation is much bigger than others, and with time increases the discharge deviation increases.

Fig. 9 shows the emitter discharge deviation in the air and soil under different *H*. It can be seen that the emitter discharge deviations decrease with the increase of *H*, and the discharge variations in the air and soil are different. When *H* is less than 20 cm, the discharge deviation in the soil decreases rapidly with *H*, when *H* is higher than 20 cm, the discharge deviation would change more smoothly. However, the discharge deviation in the air will keep decreasing with increasing *H*. When *H* of the ceramic emitter is higher than 19 cm, the discharge deviation in the soil is smaller than that in the air. Therefore, when *H* is smaller than a threshold value, the discharge deviation of the ceramic emitter in the soil would be greater than that in the air. This means that when *H* is higher than the fixed value, the soil will play a critical role in balancing the outflow of the emitter, such that the discharge deviation is reduced. To reduce the discharge deviation, the working pressure head of the emitter should be higher than a threshold value (about 19 cm).

According to the regulations of ASABE, the discharge deviation under *H* of 10 cm for both types of emitters is not acceptable. When *H* is greater than or equal to 20 cm, the discharge deviations in the soil are less than 30 %, and the discharge deviation in the soil is less than that in the air. For example, when *H* is 50 cm, the discharge deviation of CE2 is about 3.5 % in the soil, and the discharge deviation in the air is 22.7 %.

Fig. 10 shows the change of soil water content uniformity with time under different treatments over 360 min. Soil water content uniformities are all higher than 80 % when *H* is 20 cm and 50 cm. The

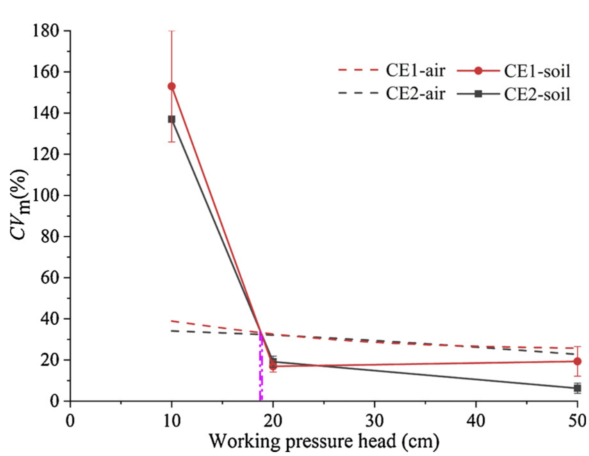


**Fig. 9.** Relationship between discharge deviation and *H*.

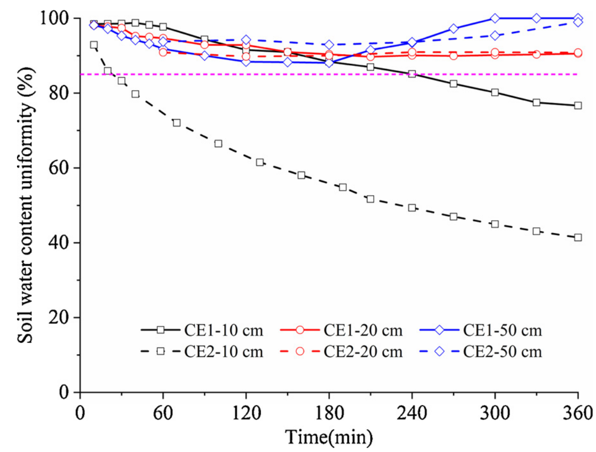


**Fig. 10.** Soil water content uniformity as a function of time at different *H* and emitter types.

higher the *H*, the higher the soil water content uniformity. However, the soil water content uniformity decreases from the initial 100 % to less than 80 % when *H* is 10 cm.

## 4. Discussion

### 4.1. The difference between SICE and SDI

Various features of SICE and SDI are relevant to compare. The discharge of SDI might be affected by the soil water potential; however, the working pressure head of SDI is generally 1000 cm, and the discharge is greater than 0.4 L $h^{-1}$. Due to its large discharge and small orifice of SDI, a positive pressure region would form at the orifice in general. Shani et al. (1996); Warrick and Shani (1996) found that soil water potential became positive in the soils with a lower infiltration capacity (compared with the emitter discharge in the air), and a small pressure difference across the emitter led to the discharge of the emitter decreasing. Thebaldi et al. (2016) found that positive backpressure reduced emitter discharge, and non-pressure compensating emitters had a corresponding decrease in the discharge exponent; in the pressure-compensating emitter, the emitter discharge increased. If the emitter exponent of the ceramic emitter is 1, and the *H* is less than 50 cm, then positive backpressure builds in the soil, and the emitter discharge changes substantially. Therefore, due to backpressure, the discharge of non-pressure compensating emitters will change significantly.

Saefuddin et al. (2019) designed a new ring-shaped emitter, and the working pressure head was kept constant at 1 cm and 5 cm to avoid a build-up in positive backpressure at the outlets of the emitter. The ceramic emitter is a non-pressure compensating emitter. When the emitter discharge coefficient is large (such as CE1), the emitter's discharge ratio of soil to air is 71 % and 75 % under *H* of 20 cm and 50 cm, respectively. To avoid the influence of positive pressure on the emitter discharge, *H* should be as small as possible. When the emitter discharge coefficient is small (such as CE2), with the increase of *H* the emitter discharge ratio of soil to air decreases from 190 % to 109 %. To make use of the effect of soil water potential on the outflow of the emitter, *H* also should have a smaller value. However, when *H* is 10 cm, the emitter cannot flow normally. Therefore, to reduce the inhibitory effect of the soil positive pressure, and use the soil's promotion effect on the emitter discharge, the working pressure head should be a relatively small value (but higher than 10 cm).

### 4.2. The difference between SICE and pitcher irrigation

Pitcher irrigation is still widely used in arid and semi-arid regions, such as in Iran, India, and Jordan (Gopinath and Veeravalli, 2011; Singh et al., 2011; Tesfaye et al., 2011). The irrigation water seeps through micropores inside the pitcher and enters the soil near the roots of the crop, therefore this irrigation method has very high water use efficiency. Batchelor et al. (1996) conducted irrigation experiments (1985–1995) and found that subsurface irrigation with clay pipes was a particularly effective method in improving crop yields, quality, and water use efficiency, as well as being inexpensive, simple, and easy to use. Abu-Zreig et al. (2018) used seven ceramic pots with various dimensions to evaluate water seepage rates under various environmental and hydraulic conditions. The experiments revealed that ceramic pitchers can be used to supply water even under negative pressure head, thus eliminating the need for pressurized flow inside irrigation pipes.

Water is the main factor restricting the growth of crops in arid areas, and increasing yield and saving water can even be achieved using a pot with a large deviation. Siyal et al. (2016) used clay pots with permeability coefficients 0.114 and 0.060 cm/d, with the surface area of both pots close to 3000 $cm^2$. Abu-Zreig and Atoum (2004) used 14 clay pots that had a permeability coefficient in the range 0.022–0.237 cm/d, and a surface area $1120-1835\ cm^2$. The relationship between discharge and the permeability coefficient was linear, the discharge of clay pots generally low, and the water seepage area large; as such, a small difference in the permeability coefficient may lead to a substantial change in the discharge of the clay pot. Therefore, to ensure the quality of irrigation, smaller manufacturing deviations are needed and *H* of clay pots need to be increased. In this study, when *H* of the ceramic emitter is lower than 20 cm, the discharge deviation in the soil increased. Therefore, to reduce the discharge deviation and ensure the irrigation quality, *H* of the ceramic emitter must be greater than 20 cm.

### 4.3. Irrigation quality index of SICE

Irrigation uniformity is one of the most important indexes in the design and management of irrigation systems (Patel and Rajput, 2009). Irrigation uniformity is calculated by measuring the emitter discharge and using Christiansen's formula. It is also possible to measure the pressure distribution on the capillary, calculate the discharge through the pressure-discharge relationship of the emitter, and then calculate uniformity (Gil et al., 2008). However, because subsurface irrigation pipes and emitters are buried in the ground, discharge and pressure are difficult to measure. Also, the emitter discharge in the soil is generally different from that in the air, so evaluation of the uniformity of subsurface irrigation is difficult (Rodriguez-Sinobas et al., 2009). The irrigation system delivers water to the soil through the emitter, and the crop absorbs water from the soil, so the soil water content uniformity can better represent irrigation quality. It can be seen from **Fig. 10** when *H* is higher than 20 cm, the soil water content uniformity is higher than 80 %, therefore the irrigation quality is "good" according to ASABE standards. However, when the discharge deviation in the soil is 6.27–19.16 %, the performance of the emitter is unacceptable according to ASABE standards. Therefore, soil water content uniformity would be a suitable index to evaluate the irrigation quality of SICE.

Many factors affect soil water content uniformity, such as discharge and manufacturing deviation of the emitter, soil spatial variability, and spacing of emitters (Li et al., 2012; Ren et al., 2018, 2017; Wang et al., 2016). Rodriguez-Sinobas et al. (2012) found that water application uniformity was good for both drip and subsurface drip irrigation methods. Zhou et al. (2018) found that drip lateral spacing and mulching methods imposed no significant effect on uniformity. The higher the *H*, the higher the uniformity. When *H* is less than 20 cm, the soil water content uniformity shows a decreasing trend with time, and it will be less than 80 % after a certain time interval. Therefore, to ensure the uniform growth of crops, the working pressure head of SICE must be higher than 20 cm.

## 5. Conclusions

In this paper, laboratory experiments were conducted to study ceramic emitter hydraulic characteristics in the air and soil under different working pressure heads and emitter types. The study demonstrated that when *H* increased in the air, the emitter discharge increased linearly, and the discharge deviation decreased. With increased *H* in the soil, the emitter discharge, soil water content, and soil water content uniformity increased, whereas the discharge deviation in the soil decreased gradually. When the emitter discharge coefficient was larger, the emitter discharge gradually decreased, and the discharge in the soil would stabilize and then eventually be less than the emitter discharge. When the emitter discharge coefficient was small, the emitter discharge in the soil would be larger than in the air. When *H* was greater than or equal to 20 cm, the discharge deviation in the soil was less than that in the air, and the soil water content uniformity was higher than 80 %. The soil water content uniformity could be used in the evaluation of the irrigation quality of SICE, as based on reliability and overall convenience of observation. To effectively use soil water potential on the outflow of the emitter, reduce the discharge deviation, and improve soil water content uniformity, the working pressure head of SICE should be higher than 20 cm. This research should help inform future designs of similar irrigation systems.

## Declaration of Competing Interest

The authors declared that they have no conflicts of interest to this work.

## Acknowledgments

The authors gratefully acknowledge the National Natural Science Foundation of China (551879225), CAS "Youth Scholar of West China" Program (XAB2019B09), the Key Research and Development Program of Ningxia Hui Autonomous Region (2018BBF02006), the National Science and Technology Support Program (2015BAD22B01-02), and the Fundamental Research Funds for the Central Universities (2452019194).

## References

Abu-Zreig, M.M., Atoum, M.F., 2004. Hydraulic characteristics and seepage modelling of clay pitchers produced in Jordan. Can. Biosyst. Eng. 46, 1–15.
Abu-Zreig, M., Zraiqat, A., Abd Elbasit, M., 2018. Seepage rate from ceramic pitchers under positive and negative hydraulic head. Appl. Eng. Agric. 34 (4), 707–714.
Adu, M.O., Yawson, D.O., Abano, E.E., Asare, P.A., Armah, F.A., Opoku, E.K., 2019. Does water-saving irrigation improve the quality of fruits and vegetables? Evidence from meta-analysis. Irrig. Sci. 37 (6), 669–690.
ASABE, 2006. Field evaluation of microirrigation systems. Asabe Standards American Society of Agricultural and Biological Engineers. St. Joseph, Michigan.
Bainbridge, D.A., 2001. Buried clay pot irrigation: a little known but very efficient traditional method of irrigation. Agric. Water Manag. 48 (2), 79–88.
Batchelor, C., Lovell, C., Murata, M., 1996. Simple microirrigation techniques for improving irrigation efficiency on vegetable gardens. Agric. Water Manag. 32 (1), 37–48.
Cai, Y., Wu, P., Zhang, L., Zhu, D., Chen, J., Wu, S., Zhao, X., 2017. Simulation of soil water movement under subsurface irrigation with porous ceramic emitter. Agric. Water Manag. 192, 244–256.
Cai, Y., Wu, P., Zhang, L., Zhu, D., Wu, S., Zhao, X., Dong, Z., 2018. Prediction of flow characteristics and risk assessment of deep percolation by ceramic emitters in loam. J. Hydrol. 566, 901–909.
Cai, J., Fan, S., Liu, F., Jiang, W., Wu, H., Fan, Z., 2019a. Preparation of porous $Al_2O_3$ ceramic microspheres by a novel micro-droplet jetting rapid forming method. Ceram. Int. 45 (16), 20583–20588.
Cai, Y., Zhao, X., Wu, P., Zhang, L., Zhu, D., Chen, J., Lin, L., 2019b. Ceramic patch type subsurface drip irrigation line: construction and hydraulic properties. Biosyst. Eng. 182, 29–37.
Camp, C.R., 1998. Subsurface drip irrigation: a review. Trans. ASAE 41 (5), 1353–1367.
Christiansen, J.E., 1941. The uniformity of application of water by sprinkler systems. Agric. Eng. 22, 89–92.
Gardner, W.R., 1958. Some steady state solutions of unsaturated moisture flow equations with application to evaporation from a water table. Soil Sci. 85, 228–232.
Gil, M., Rodriquez-Sinobas, L., Juana, L., Sanchez, R., Losada, A., 2008. Emitter discharge

variability of subsurface drip irrigation in uniform soils: effect on water-application uniformity. Irrig. Sci. 26 (6), 451–458.
Gopinath, K., Veeravalli, S.V., 2011. Auto-regulative capability of pot/pitcher irrigation. J. Sci. Ind. Res. 70 (8), 656–663.
Hajjaji, M., Mezouari, H., 2011. A calcareous clay from Tamesloht (Al Haouz, Morocco): properties and thermal transformations. Appl. Clay Sci. 51 (4), 507–510.
Kaltsas, A.M., Mamolos, A.P., Tsatsarelis, C.A., Nanos, G.D., Kalburtji, K.L., 2007. Energy budget in organic and conventional olive groves. Agric. Ecosyst. Environ. 122 (2), 243–251.
Lamm, F.R., Trooien, T.P., 2003. Subsurface drip irrigation for corn production: a review of 10 years of research in Kansas. Irrig. Sci. 22 (3-4), 195–200.
Lazarovitch, N., Shani, U., Thompson, T.L., Warrick, A.W., 2006. Soil hydraulic properties affecting discharge uniformity of gravity-fed subsurface drip irrigation systems. J. Irrig. Drain. Eng. 132 (6), 531–536.
Li, J., Zhao, W., Yin, J., Zhang, H., Wen, J., 2012. The effects of drip irrigation system uniformity on soil water and nitrogen distributions. Trans. Asabe 55 (2), 415–427.
Li, Y., Wang, L., Xue, X., Guo, W., Xu, F., Li, Y., Chen, F., 2017. Comparison of drip fertigation and negative pressure fertigation on soil water dynamics and water use efficiency of greenhouse tomato grown in the North China Plain. Agric. Water Manag. 184, 1–8.
Li, Y., Xue, X., Guo, W., Wang, L., Duan, M., Chen, H., Chen, F., 2019a. Soil moisture and nitrate-nitrogen dynamics and economic yield in the greenhouse cultivation of tomato and cucumber under negative pressure irrigation in the North China Plain. Sci. Rep. 9.
Li, Y., Yang, X., Liu, D., Chen, J., Zhang, D., Wu, Z., 2019b. Permeability of the porous Al2O3 ceramic with bimodal pore size distribution. Ceramics Int. 45, 5952–5957.
Liu, H.H., Birkholzer, J., 2012. On the relationship between water flux and hydraulic gradient for unsaturated and saturated clay. J. Hydrol. 475, 242–247.
Min, F., Song, H., Zhang, N., 2018. Experimental study on fluid properties of slurry and its influence on slurry infiltration in sand stratum. Appl. Clay Sci. 161, 64–69.
Naik, B.S., Panda, R.K., Nayak, S.C., Sharma, S.D., Sahu, A.P., 2013. Impact of pitcher material and salinity of water used on flow rate, wetting front advance, soil moisture and salt distribution in soil in pitcher irrigation: a laboratory study. Irrig. Drain. 62 (5), 687–694.
Nalliah, V., Ranjan, R.S., 2010. Evaluation of a capillary-irrigation system for better yield and quality of hot pepper (*Capsicum annuum*). Appl. Eng. Agric. 26 (5), 807–816.
Pachpute, J.S., 2010. A package of water management practices for sustainable growth and improved production of vegetable crop in labour and water scarce Sub-Saharan Africa. Agric. Water Manag. 97 (9), 1251–1258.
Paredes, A.M.D., San Jose, J.D., 2019. Pitcher irrigation: some theoretical and practical aspects. Irrig. Drain. 68 (3), 542–550.
Patel, N., Rajput, T.B.S., 2009. Effect of subsurface drip irrigation on onion yield. Irrig. Sci. 27 (2), 97–108.
Powell, J.W., Welsh, J.M., Pannell, D., Kingwell, R., 2019. Can applying renewable energy for Australian sugarcane irrigation reduce energy cost and environmental impacts? A case study approach. J. Clean. Prod. 240, 118177.
Prada, A., Civan, F., 1999. Modification of Darcy's law for the threshold pressure gradient. J. Pet. Sci. Eng. 22, 237–240.
Ren, C., Zhao, Y., Wang, J., Bai, D., Zhao, X., Tian, J., 2017. Lateral hydraulic performance of subsurface drip irrigation based on spatial variability of soil: simulation. Agric. Water Manag. 193, 232–239.
Ren, C., Zhao, Y., Dan, B., Wang, J., Gong, J., He, G., 2018. Lateral hydraulic performance of subsurface drip irrigation based on spatial variability of soil: experiment. Agric. Water Manag. 204, 118–125.
Rodriguez-Sinobas, L., Gil, M., Juana, L., Sanchez, R., 2009. Water distribution in laterals and units of subsurface drip irrigation. Ii: field evaluation. J. Irrig. Drain. Eng. 135 (6), 729–738.
Rodriguez-Sinobas, L., Gil, M., Sanchez, R., Benitez, J., 2012. Evaluation of drip and subsurface drip irrigation in a uniform loamy soil. Soil Sci. 177 (2), 147–152.
Romero-Gamez, M., Castro-Rodriguez, J., Suarez-Rey, E.M., 2017. Optimization of olive growing practices in Spain from a life cycle assessment perspective. J. Clean. Prod. 149, 25–37.
Wang, S., Zhu, W., Fei, K., He, H., Fu, G., Shu, S., Song, J., 2019. COD (glucose configuration) effects on the non-Darcy flow of compacted clay in a municipal solid waste landfill. Waste Manag. 84, 220–226.
Saefuddin, R., Saito, H., Simunek, J., 2019. Experimental and numerical evaluation of a ring-shaped emitter for subsurface irrigation. Agric. Water Manag. 211, 111–122.
Sampson, G.S., Perry, E.D., 2019. Peer effects in the diffusion of water-saving agricultural technologies. Agric. Econ. 50 (6), 693–706.
Shani, U., Xue, S., GordinKatz, R., Warrick, A.W., 1996. Soil-limiting flow from subsurface emitters, I: pressure measurements. J. Irrig. Drain. Eng. 122 (5), 291–295.
Singh, R.K., Ghosal, S., 2015. Effect of pitcher fertigation on shooting response and kusmi lac crop performance on ber (*Ziziphus mauritiana*). Natl. Acad. Sci. Lett. India 38 (5), 379–382.
Singh, P., Jaipal, P.R., Vasudevan, P., Sen, P.K., Jangir, R.P., 2011. Buried clay pot irrigation for horticulture in arid zones: a case study. J. Sci. Ind. Res. 70 (8), 709–712.
Siyal, A.A., van Genuchten, M.T., Skaggs, T.H., 2009. Performance of pitcher irrigation system. Soil Sci. 174 (6), 312–320.
Siyal, A.A., Siyal, A.G., Siyal, P., Solangi, M., Khatri, I., 2016. Pitcher irrigation: effect of pitcher wall properties on the size of soil wetting front. Sci. Int. 28 (2), 1299–1304.
Su, L., Wang, Q., Shan, Y., Zhou, B., 2016. Estimating soil saturated hydraulic conductivity using the Kostiakov and Philip infiltration equations. Soil Sci. Soc. Am. J. 80 (6), 1463.
Tesfaye, T., Tesfaye, K., Woldetsadik, K., 2011. Clay pot irrigation for tomato (Lycopersicon esculentum Mill) production in the north east semiarid region of Ethiopia. J. Agric. Rural Dev. Tropics Subtropics 112 (1), 11–18.
Thebaldi, M.S., Lima, L.A., de Almeida, W.F., Andrade, R.R., 2016. Backpressure effects on the flow-pressure relation of driplines. Engenharia Agricola 36 (1), 55–62.
Todde, G., Murgia, L., Deligios, P.A., Hogan, R., Carrelo, I., Moreira, M., 2019. Energy and environmental performances of hybrid photovoltaic irrigation systems in Mediterranean intensive and super-intensive olive orchards. Sci. Total Environ. 651, 2514–2523.
van Genuchten, M.T., 1980v. A closed-form equation for predicting the hydraulic conductivity of unsaturated soils. Soil Sci. Soc. Am. J. 44 (5), 892–898.
Vasudevan, P., Thapliyal, A., Sen, P.K., Dastidar, M.G., Davies, P., 2011. Buried clay pot irrigation for efficient and controlled water delivery. J. Scientific Ind. Res. 70 (8), 645–652.
Vasudevan, P., Thapliyal, A., Tandon, M., Dastidar, M.G., Sen, P.K., 2014. Factors controlling water delivery by pitcher irrigation. Irrig. Drain. 63 (1), 71–79.
Wang, W., Zhuo, L., Li, M., Liu, Y.L., Wu, P.T., 2019b. The effect of development in water-saving irrigation techniques on spatial-temporal variations in crop water footprint and benchmarking. J. Hydrol. 577, 123916.
Wang, J., Zhu, D.L., Bralts, V.F., Zhang, L., 2016. Hydraulic analysis of looped micro-irrigation submain units using the finite element method. Trans. Asabe 59 (3), 909–923.
Warrick, A.W., Shani, U., 1996. Soil-limiting flow from subsurface emitters, II: effect on uniformity. J. Irrig. Drain. Eng. 122 (5), 296–300.
Wu, Z., Li, Y., Sun, X., Li, M., Jia, R., 2018. Experimental study on the gas phase permeability of montmorillonite sediments in the presence of hydrates. Mar. Pet. Geol. 91, 373–380.
Zhang, G., Chen, H., Yang, S., Guo, Y., Li, N., Zhou, H., 2018. Frozen slurry-based laminated object manufacturing to fabricate porous ceramic with oriented lamellar structure. J. Eur. Ceram. Soc. 38 (11), 4014–4019.
Zhou, L., He, J., Qi, Z., Dyck, M., Zou, Y., Zhang, T., 2018. Effects of lateral spacing for drip irrigation and mulching on the distributions of soil water and nitrate, maize yield, and water use efficiency. Agric. Water Manag. 199, 190–200.